A conduction velocity adapted eikonal model for electrophysiology problems with re-excitability evaluation

Cesare Corrado, Nejib Zemzemi

A conduction velocity adapted eikonal model for electrophysiology problems with re-excitability evaluation

Cesare Corrado[a,*], Nejib Zemzemi[b,c]

[a]*Division of Imaging Sciences & Biomedical Engineering, King's College London, London SE17EH, United Kingdom*
[b]*Inria Bordeaux Sud-Ouest, Carmen team, Avenue de la Vieille Tour, Talence 33000, France*
[c]*IHU-LIRYC, avenue du Haut Lévèque 33600 Pessac, France*

Abstract

Computational models of heart electrophysiology achieved a great interest from the medical community since they represent a novel framework to study the mechanisms that underpin heart pathologies. The high demand of computational resources and the long computational times required to evaluate the model solution hamper the use of detailed computational models in clinical applications. In this paper, we propose a multi-front eikonal algorithm capable of adapting the conduction velocity (CV) to the activation frequency of the tissue substrate. We then couple the new eikonal model with a Mitchell-Schaeffer (MS) ionic model to determine the tissue electrical state. Compared to the standard eikonal model, this model introduces three novelties: first, the local value of the transmembrane potential and of the ionic variable are known from the solution of the ionic model; second, the action potential duration (APD) and the diastolic interval (DI) are computed from the solution of the MS model and used to determine when a part of the tissue is re-excitable. Third, CV is locally adapted to the underpinning electrophysiological state through the analytical CV restitution expression and the computed local DI. We conduct

*Corresponding author
Email addresses: cesare.corrado@kcl.ac.uk (Cesare Corrado), nejib.zemzemi@inria.fr (Nejib Zemzemi)

series of simulations on a tissue slab and on 3D realistic heart geometry and compare results to the monodomain. Our results show that the new model is much more accurate than the standard eikonal model. This model enables the numerical simulation of the heart electrophysiology on a clinical time scale and thus constitutes a good model candidate for computer-guided cardiac therapy.
Keywords: Cardiac Electrophysiology, Multi-front Eikonal model, Dijkstra algorithm, Mitchell And Schaeffer model, Clinical time scale, Conduction velocity

---

1. Introduction

The propagation of an electrical stimulus in the cardiac tissue is mathematically described by the bidomain model Tung (1978); Clements et al. (2004), that is a system of a parabolic reaction-diffusion and an elliptic PDEs describing the electrical state of an intracellular and extracellular continuum media, separated by the cell membrane. The electrical state of the cell membrane that characterises the reaction term, is described by a non-linear system of ODEs, that either describes the flux of the ion species across the cell membrane (biophysical ionic models, Ten Tusscher et al. (2004); Luo & Rudy (1991, 1994)), or that tries to reproduce the shape of the action potential (phenomenological ionic models, Mitchell & Schaeffer (2003); Aliev & Panfilov (1996)). When intracellular and extracellular conductivity tensors are considered proportional up to a given constant, it is possible to simplify the bidomain description with the so-called mono-domain approximation Clements et al. (2004), that is characterised by only a parabolic non-linear reaction-diffusion PDE. Even though computationally improved, the mono-domain simplification still requires solving a non-linear system that arises from the numerical discretization. Since the characteristic space and time scales of the electrophysiology are small if compared to the standard left ventricle dimensions ($h \approx 100\,\mu$m, $L \approx 10\,$cm) and cycle length ($dt \approx 0.1\,$ms, $T \approx 700\,$ms) also the computational demand of the monodomain simplification is still too high in view of clinical applications, where the

time is one of the principal constraints. Approaches based on proper orthogonal decompositions (POD) were applied to the bidomain model, furnished good results in terms of performances Corrado et al. (2016a) and allowed to cope with state corrections on electrophysiology data assimilation Corrado et al. (2015). However, the requirement to build a data set of snapshot limits their application to domains with strong heterogeneities.

The eikonal model describes the propagation of an electrical stimulus from a region Γ of the cardiac tissue domain Ω_H in terms of isochronous surfaces. Thus, the eikonal model captures the propagation of the activation front, when the propagation velocity is known. Due to the causality of the propagation front, the eikonal equation can be solved in a very efficient way, either by fast marching methods (FMM) Sethian (1996) or by Dijkstra algorithm Wallman et al. (2012). The required computational time and resources enable its to be an optimal candidate in view of clinical applications. In this work we adopt the Dijkstra algorithm for the numerical solution of the eikonal equation, since was proven to be a very effective algorithm, Wallman et al. (2012). We suitably modify that algorithm to take into account of the multi-front activations, Wallman et al. (2013); Pernod et al. (2011); Sermesant et al. (2007) and the CV variations related to the tissue electrophysiology. We describe the cell membrane action potential with the MS model Mitchell & Schaeffer (2003) and we adopt the asymptotic expression introduced in Cain et al. (2004) to locally adapt CV to the heart rate. The work is organised as follows: in section 2 we introduce the monodomain MS ionic model and its restitution properties; in section 3 we introduce the modified eikonal model and its algorithm pseudo-code. In section 4 we describe the proposed Eikonal MS algorithm; in section 5 we apply the proposed algorithm to a tissue slab and to a ventricular geometry obtained by CT segmentation and we compare the solution with those either obtained by the mono-domain model or by the Eikonal MS with a CV independent of the heart rate.

2. The Monodomain Mitchell and Schaeffer model

The MS ionic model Mitchell & Schaeffer (2003) is a two state variable ODE system that describes the ionic fluxes across the cell membrane with a gated-inward and an ungated outward ionic current. When incorporated into a tissue Ω_H with boundary Σ and for a time interval $[0, T]$, the MS mono-domain model leads to the following system:

$$
\begin{aligned}
&A_{\mathrm{m}}\left(C_{\mathrm{m}}\partial_t V_{\mathrm{m}} + \beta I_{\mathrm{ion}}(V_{\mathrm{m}}, \mathrm{h})\right) - \mathrm{div}(\underline{\underline{D}}_{\mathrm{m}}\underline{\nabla} V_{\mathrm{m}}) = A_{\mathrm{m}} I_{\mathrm{app}}, && \text{in } \Omega_H \times (0,T),\\
&\partial_t \mathrm{h} + g(V_{\mathrm{m}}, \mathrm{h}) = 0, && \text{in } \Omega_H \times (0,T),\\
&\underline{\underline{D}}_{\mathrm{m}} \nabla V_{\mathrm{m}} \cdot n = 0, && \text{on } \Sigma,
\end{aligned}
$$

$$
\begin{aligned}
I_{\mathrm{ion}}(V_{\mathrm{m}}, \mathrm{h}) &= -\frac{\mathrm{h}\left(V_{\mathrm{m}} - V_{\mathrm{min}}\right)^2 \left(V_{\mathrm{max}} - V_{\mathrm{m}}\right)}{\tau_{\mathrm{in}}\left(V_{\mathrm{max}} - V_{\mathrm{min}}\right)^3} + \frac{\left(V_{\mathrm{m}} - V_{\mathrm{min}}\right)}{\tau_{\mathrm{out}}\left(V_{\mathrm{max}} - V_{\mathrm{min}}\right)},\\
g(V_{\mathrm{m}}, \mathrm{h}) &= \begin{cases} \frac{\mathrm{h}-1}{\tau_{\mathrm{open}}}, & \text{if } V_{\mathrm{m}} \le V_{\mathrm{gate}},\\ \frac{\mathrm{h}}{\tau_{\mathrm{close}}}, & \text{if } V_{\mathrm{m}} > V_{\mathrm{gate}}, \end{cases}
\end{aligned}
\tag{1}
$$

where V_{m} is the transmembrane potential, h is the gating variable of the inward current, V_{min}, V_{max} are the minimum and the maximum characteristic values of the transmembrane potential, C_{m} is the membrane capacitance per area unit, β is a reaction factor, typically $\beta = C_{\mathrm{m}}\left(V_{\mathrm{max}} - V_{\mathrm{min}}\right)$, A_{m} is the cell surface per volume unit, $\underline{\underline{D}}_{\mathrm{m}}$ is the bulk conductivity, I_{app} is an external stimulus triggering the activation, V_{gate} is the gate potential where inward channels switch between open and close, and τ_{in}, τ_{out}, τ_{open} and τ_{close} are the 4 time constants characterising the four phases of the action potential. When the tissue is activated, the transmembrane potential shows an upstroke. For a single activation, the elapsed time such as $V_{\mathrm{m}} \ge V_{\mathrm{gate}}$ is defined as the action potential duration (APD), while for two consecutive activations the elapsed time such as $V_{\mathrm{m}} < V_{\mathrm{gate}}$ is defined as the diastolic interval (DI). According to Mitchell & Schaeffer (2003), it is possible to express the APD at the $n+1$-th beat as a function of DI at the

n-th beat, with the following leading order approximation:

$$
\begin{aligned}
&APD_{n+1}\left(DI_n\right) = \tau_{\text{close}} \log\left(\frac{h\left(DI_n\right)}{h_{\min}}\right),\\
&h_{\min} = 4\frac{\tau_{\text{in}}}{\tau_{\text{out}}},\\
&h\left(DI_n\right) = 1 - \left(1 - h_{\min}\right) e^{-\frac{DI_n}{\tau_{\text{open}}}}.
\end{aligned}
$$

In order to obtain a restitution for CV, we first define the diffusivity tensor as:

$$\sigma_{\text{m}} = \frac{\underline{\underline{D}}_{\text{m}}}{A_{\text{m}} C_{\text{m}}},$$

with a longitudinal component σ_{m}^{l}, parallel to the local fibre direction $\vec{a}$ and transversal one σ_{m}^{t}, and then re-arrange it as follows:

$$\sigma_{\text{m}} = \sigma_{\text{m}}^{t}\underline{\underline{I}} + \left(\sigma_{\text{m}}^{l} - \sigma_{\text{m}}^{t}\right)\vec{a}\otimes\vec{a} = \sigma_{\text{m}}^{l}\left(\rho\underline{\underline{I}} + \left(1-\rho\right)\vec{a}\otimes\vec{a}\right) = \sigma_{\text{m}}^{l}\underline{\underline{D}} \tag{2}$$

where $\rho = \sigma_{\text{m}}^{t}/\sigma_{\text{m}}^{l} \leq 1$ is the ratio between the transversal and longitudinal diffusivity components and $\underline{\underline{D}}$ is a dimensionless tensor that describes the tissue anisotropy. In Cain et al. (2004) a restitution relation on CV is introduced for a 1D filament. In this work introduce the simplifying hypothesis that the ratio between transversal and longitudinal components of CV is equal to ρ and does not vary with the frequency; thus, we adopt the following relation for the longitudinal component:

$$CV_{n+1}\left(DI_n\right) = \frac{1}{4}\left(3\sqrt{h\left(DI_n\right) - h_{\min}} - \sqrt{h\left(DI_n\right)}\right)\sqrt{\frac{2\sigma_{\text{m}}^{l}}{\tau_{\text{in}}}}. \tag{3}$$

Remark. *In multi-dimension problems (2D, 3D), the conductivity tensor $\underline{\underline{D}}$ has two eigenvalues: the former is equal to* 1 *and corresponds to the conductivity in the fibre direction; the second is equal to ρ that corresponds to the conductivity in the transverse direction. If $\rho = 1/2$ for instance, the CV is $\sqrt{2}$ faster than it should be in the transverse direction. We take into account this issue in the next paragraph.*

3. The Eikonal model for the activation

The eikonal equation describes the propagation of an electrical wavefront generated on a region Γ and through a non-homogeneous anisotropic continuum Ω_H. Denoting with $T_{\text{act}}(\vec{x})$ the time at which the wavefront reaches the point $\vec{x}$ and with $F(\vec{x})$ the characteristic velocity the wavefront propagates in the medium, the eikonal equation reads as follows:

$$\begin{cases} F\sqrt{(\underline{\nabla} T_{\text{act}})^{\intercal}\, \underline{\underline{D}}\, \underline{\nabla} T_{\text{act}}} = 1 & \text{on } \Omega_H \\ T_{\text{act}} = 0 & \text{on } \Gamma \end{cases} \tag{4}$$

where $\underline{\underline{D}}$ is the tensor introduced in (2) that takes into account of the propagation anisotropy. To obtain the same conduction velocity values in the eikonal model and in the monodomain Mitchell and Schaeffer model, from (3) and (4) it follows:

$$\begin{aligned} F &= \alpha\sqrt{\frac{2\sigma_{\text{m}}^{l}}{\tau_{\text{in}}}} \\ \alpha(DI_n) &= \frac{1}{4}\left(3\sqrt{h\left(DI_n\right) - h_{\min}} - \sqrt{h\left(DI_n\right)}\right) \end{aligned} \tag{5}$$

Once the space distribution $DI_n(\vec{x})$ is known, it is possible to determine the activation times for a particular electrical state of the medium by solving the eikonal equation (4). In this paper, the eikonal equation is solved using a Dijkstra algorithm Wallman et al. (2012) which has been modified in order to take into account of the presence of re-excitable regions Wallman et al. (2013); Pernod et al. (2011); Sermesant et al. (2007) and of the local variations on CV. Differently from Wallman et al. (2013); Pernod et al. (2011), in this paper, we solve numerically the ionic MS model on each node of the graph, we use the computed solution to determine whether the point is re-excitable, its value of DI and we adapt the propagation velocity of the medium to the electrophysiological state of the tissue through DI. This has many advantages. First, it allows taking into account of the spatial heterogeneity of the parameters that characterise the ionic model and thus of their high impact on the electrical wave propagation; the heterogeneity of the parameter characterising the ionic model can be considered nodal-wise. Second, it allows determining DI on each

node of the mesh since the transmembrane potential is computed. Third, the adaptation of CV and the re-excitability criterion allow taking into account of slowing in the propagation and of functional blocks: when the electrical wave fails to propagate in the tissue especially in the refractory period. Following Wallman et al. (2012), we denote by n_0 the set of points belonging to Γ, by Q the priority queue where a set of trial points are ordered with respect to their candidate activation time and by P_{visited} the container of points with a definitely determined activation time. These variables are initialized as described in Algorithm 1. In order to compute the time that takes the electrical wave to

Algorithm 1 Initialization of the multi-frontal eikonal

$Q \rightarrow Q \cup n_0,\ n_0 \in \Gamma$

$T_{\text{act}}(n_0) = 0$

$T_{\text{act}}(n \notin \Gamma) = \infty$

$P_{\text{visited}}\,(n_0) = \text{true}$

$t_{cur} = 0$

propagate from a node n_i characterised by its position $\vec{x}_i$ to a neighbour node n_j characterised by its position $\vec{x}_j$ we define the cost function $c_{ij}\left(DI_{n_i}, DI_{n_j}\right)$ as follows:

$$\begin{cases} c_{ij}\left(DI_{n_i}, DI_{n_j}\right) = \sqrt{\vec{v}_{ij}^{\intercal}\underline{\underline{D}}^{-1}\vec{v}_{ij}}/\left(F\left(DI_{n_i}, DI_{n_j}\right)/\delta\right), \\ \vec{v}_{ij} = \vec{v}(n_i, n_j) = \vec{x}_j - \vec{x}_i, \end{cases} \tag{6}$$

where δ is a corrective coefficient Wallman et al. (2012); Kim & Hespanha (2003) that compensates the error introduced by the graph representation of the domain. The characteristic velocity $F\left(DI_{n_i}, DI_{n_j}\right)$ along a segment $\vec{v}_{ij}$ depends on the values of the diasotlic interval at both vertices of the edge, through the parameter $\alpha\left(DI_{n_i}, DI_{n_j}\right)$. In this work, we choose the following relation:

$$\alpha\left(DI_{n_i}, DI_{n_j}\right) = \max\left(0, \max(\alpha\left(DI_{n_i}\right), \alpha\left(DI_{n_j}\right))\right) \tag{7}$$

Introducing a time step dt, it is possible to evaluate the set of points that

are activated until the time $t^n = n\text{dt}$ and their corresponding activation time by applying Algorithm 2, where the function $\text{TIME}\,(n_i, n_j)$ is defined as follows:

$$\text{TIME}\,(n_j, n_i) = \min\left(T_{\text{act}}(n_i), T_{\text{act}}(n_j) + c_{ij}\left(DI_{n_i}, DI_{n_j}\right)\right) \tag{8}$$

For each node n in the graph, we denote by $\text{NEIGH}\,(n)$ the set of points that are connected with n; these points correspond to the mesh points sharing an edge with n.

Algorithm 2 Eikonal Algorithm with time stepping

while $Q \neq \phi$ or $t_{cur} \leq \bar{t}$ **do**
  $n = argmin_{n \in Q} T_{\text{act}}(n)$
  $t_{cur} = T_{\text{act}}(n)$
  if $t_{cur} \leq \bar{t}$ **then**
    $Q = Q \backslash n$
    $P_{\text{visited}}\,(n) = \text{true}$
    for all $n_i \in \text{NEIGH}\,(n)$ **do**
      if $P_{\text{visited}}\,(n_i) = \text{false}$ **then**
        $T_{\text{act}}(n_i) = \text{TIME}\,(n, n_i)$
        $Q = Q \cup n_i$
      end if
    end for
  end if
end while

Remark. *The solution of the eikonal problem with the time stepping described in Algorithm 2 allows taking into account of multiple fronts by removing the points that became re-excitable from the container $P_{visited}$. The same time stepping also allows taking into account of the variations on CV dependent on the local electrophysiological state of the tissue. These variations are introduced into the model by modifying the characteristic propagation velocity F that determines the cost defined in (6).*

4. The Eikonal Mitchell and Schaeffer model

In this section we present two algorithms for the propagation of the electrical wave: algorithm 3, that evaluates the state variables solving the Mitchell and Schaeffer model equations at each node of the graph; algorithm 4, that adopts the leading order analytical expression of the APD restitution and furnishes, at each node, the activation times and the trans-membrane potentials through the pseudo-potentials as in Pernod et al. (2011)

Algorithm 3 is adopted in clinical applications that require the trans-membrane potential; this is the case, for example, when an electrocardiogram (ECG) or electrograms (EGM) are evaluated. Algorithm 4 is adopted in clinical applications that require narrow time constraints, such as the evaluation of the outcome of a RadioFrequency Ablation procedure.

4.1. Algorithm with state variables computation

The eikonal model introduced in section 3 is used to mimic the conductivity of the Monodomain MS model described in section 2. First, we initialize the eikonal algorithm as described in Algorithm 1. We denote by $\mathrm{N_x}$ the number of nodes in the considered graph (or mesh). For $i = 1, \ldots, \mathrm{N_x}$, the couple $(v^0_{\mathrm{m},\mathrm{i}}, \mathrm{h}^0_{\mathrm{i}})$ is the initial state at the $i-th$ node. We denote by $I_{\mathrm{app},\mathrm{i}}\left(T^{\mathrm{i}}_{\mathrm{act}}, t_{\mathrm{stim}}\right)$ an external electrical stimulus applied to the $i-th$ node at time $T^{\mathrm{i}}_{\mathrm{act}}$ and with duration t_{stim}. The couple $(v^n_{\mathrm{m},\mathrm{i}}, \mathrm{h}^n_{\mathrm{i}})$ is the electrophysiological state at time t^n and at $i-th$ node. The Eikonal MS model is computed as described in Algorithm 3.

Algorithm 3 MS-Eikonal algorithm

Initialize state variables $(v^n_{\mathrm{m,i}}, \mathrm{h}^n_{\mathrm{i}})$.

The time each node will be activated is determined by solving the Algorithm 2.

for $n = 0, \ldots, \mathrm{N_t} - 1$ **do**

for $i = 1, \ldots, \mathrm{N_x}$ **do**

- solve the MS model between t^n and t^{n+1}

$$
\begin{aligned}
& C_{\mathrm{m}} \partial_t v_{\mathrm{m,i}} + I_{\mathrm{ion}}(v_{\mathrm{m,i}}, \mathrm{h_i}) = I_{\mathrm{app}}\left(T^i_{\mathrm{act}}, t_{\mathrm{stim}}\right) \\
& \partial_t \mathrm{h_i} + g(v_{\mathrm{m,i}}, \mathrm{h_i}) = 0 \\
& I_{\mathrm{ion}}(v_{\mathrm{m,i}}, \mathrm{h_i}) = -\frac{\mathrm{h_i}}{\tau_{\mathrm{in}}} v^2_{\mathrm{m,i}}(1 - v_{\mathrm{m,i}}) + \frac{1}{\tau_{\mathrm{out}}} v_{\mathrm{m,i}} \\
& g(v_{\mathrm{m,i}}, \mathrm{h_i}) = \begin{cases} \frac{\mathrm{h_i} - 1}{\tau_{\mathrm{open}}} & \text{if } v_{\mathrm{m,i}} \leq v_{\mathrm{gate}} \\ \frac{\mathrm{h_i}}{\tau_{\mathrm{close}}} & \text{if } v_{\mathrm{m,i}} > v_{\mathrm{gate}} \end{cases}
\end{aligned}
\tag{9}
$$

- update the local APD according to the solution $v_{\mathrm{m,i}}$.
- If $v_{\mathrm{m,i}} \leq v_{\mathrm{gate}}$ and $\mathrm{h_i} \geq h_{\min}$ the node is marked as re-excitable and removed from the list of known points (the values $P_{\mathrm{visited}}(n_i) = \mathrm{false}$), the candidate activation time is set to ∞.
- On points that are marked as excitable, for each time the value of the DI is updated as follows:

$$
DI_{\mathrm{i}} = t^{n+1} - \left(T^{\mathrm{i}}_{\mathrm{act}} + APD_{\mathrm{i}}\right)
$$

and the value of CV is updated.

end for on space

Update the activation times between t^n and t^{n+1} following Algorithm 2.

end for on time

On each node, the local value APD_{i} of the action potential duration is updated as follows. If, at time t^{n+1} the trans-membrane potential crosses the threshold $v_{\mathrm{m}} = v_{\mathrm{gate}}$ with a positive time derivative, the depolarisation time on

the i-th node is evaluated as follows:

$$t_{\mathrm{dep_{,i}}} = t^n + \frac{t^{n+1} - t^n}{v_{\mathrm{m,i}}^{n+1} - v_{\mathrm{m,i}}^n} \left(v_{\mathrm{gate}} - v_{\mathrm{m,i}}^n \right) \tag{10}$$

A flag $f_{\mathrm{dep_{,i}}}$ stopping further evaluation of $t_{\mathrm{dep_{,i}}}$ is activated; for each time iteration, the actual value of the local APD is computed as: $APD_{\mathrm{i}} = t^{n+1} - t_{\mathrm{dep_{,i}}}$. If, at time t^{n+1} the trans-membrane potential crosses the threshold $v_{\mathrm{m}} = v_{\mathrm{gate}}$ with a negative time derivative and $f_{\mathrm{dep_{,i}}}$ is active, then the depolarisation time on the i-th node is evaluated as follows:

$$t_{\mathrm{rep_{,i}}} = t^n + \frac{t^{n+1} - t^n}{v_{\mathrm{m,i}}^{n+1} - v_{\mathrm{m,i}}^n} \left(v_{\mathrm{gate}} - v_{\mathrm{m,i}}^n \right) \tag{11}$$

A flag $f_{\mathrm{rep_{,i}}}$ specifying the availability of both depolarisation and repolarisation times is activated. When both $f_{\mathrm{dep_{,i}}}$ and $f_{\mathrm{rep_{,i}}}$ are activated, the local action potential duration and new diastolic interval are evaluated:

$$APD_{\mathrm{i}} = t_{\mathrm{rep_{,i}}} - t_{\mathrm{dep_{,i}}} \tag{12}$$

$f_{\mathrm{dep_{,i}}}$ and $f_{\mathrm{rep_{,i}}}$ are then switched off and the algorithm is ready to evaluate the local APD of the next activation.

4.2. Algorithm with analytical restitution

An alternative and faster formulation to Algorithm 3 is presented in Algorithm 4, that adopts pseudo-potentials and a leading order analytical approximation for the APD. To ease the notations in the formulation introduced in this section, the indexes of the nodes will be dropped.

The duration of the refractory period is denoted by RP and evaluated as follows:

$$RP = \tau_{\mathrm{out}} \log \left(\frac{0.5}{v_{\mathrm{gate}}} \right)$$

This expression was obtained by considering that during RP, $\mathrm{h} < h_{\mathrm{min}} \ll 1$ and thus $\partial_t v_{\mathrm{m}} \simeq -\frac{v_{\mathrm{m}}}{\tau_{\mathrm{out}}}$. The value of trans-membrane potential at the beginning of the RP here was approximated with the value $v_{\mathrm{m}}^{+}(h_{\mathrm{min}}) = v_{\mathrm{m}}^{-}(h_{\mathrm{min}}) = 0.5$, on the null-clines, Mitchell & Schaeffer (2003): on this point, the phase portrait "falls of" the null-cline and the analytical approximation is still accurate,

Mitchell & Schaeffer (2003). At the end of RP, $v_{\mathrm{m}} = v_{\mathrm{gate}}$, while h can be evaluated as follows:

$$h_{\mathrm{end,RP}} = h_{\mathrm{min}} \exp\left(-\frac{RP}{\tau_{\mathrm{close}}}\right)$$

The time lapse TRR required to h to increase from $h_{\mathrm{end,RP}}$ to h_{min} is evaluated from equation (1) as follows:

$$TRR = \tau_{\mathrm{open}} \log\left(\frac{1 - h_{\mathrm{end,RP}}}{1 - h_{\mathrm{min}}}\right)$$

This value will be used as threshold for the diastolic interval to determine the tissue re-excitability.

Algorithm 4 Restitution-Eikonal algorithm

Initialize $\mathrm{h} = 1$, $v_{\mathrm{m}} = 0$ and $DI = \infty$

The time each node will be activated is determined by solving the Algorithm 2.

for $n = 0, \ldots, \mathrm{N_t} - 1$ **do**

for $i = 1, \ldots, \mathrm{N_x}$ **do**

- Determine APD and t_{rep} on nodes that become activated:

$$\begin{aligned} APD &= \tau_{\mathrm{close}} \log\left(\frac{h\left(DI\right)}{h_{\mathrm{min}}}\right) \\ t_{\mathrm{rep}} &= T_{\mathrm{act}} + APD + RP \end{aligned} \tag{13}$$

- Update $v_{\mathrm{m}}^{\mathrm{n}+1}$ and $\mathrm{h}^{\mathrm{n}+1}$ and DI:

$$DI = \begin{cases} 0.0 & \text{if } T_{\mathrm{act}} \leq t^{n+1} \leq T_{\mathrm{act}} + APD + RP \\ t^{n+1} - \left(T_{\mathrm{act}} + APD + RP\right) & \text{if } t^{n+1} \geq T_{\mathrm{act}} + APD + RP \end{cases}$$

$$\mathrm{h}^{\mathrm{n}+1} = \begin{cases} \mathrm{h}^{\mathrm{n}} \exp\left(-\frac{t^{n+1} - T_{\mathrm{act}}}{\tau_{\mathrm{close}}}\right) & \text{if } T_{\mathrm{act}} \leq t^{n+1} \leq T_{\mathrm{act}} + APD \\ h_{\mathrm{min}} \exp\left(-\frac{t^{n+1} - T_{\mathrm{act}} - APD}{\tau_{\mathrm{close}}}\right) & \text{if } T_{\mathrm{act}} + APD \leq t^{n+1} \leq T_{\mathrm{act}} + APD + RP \\ 1 + \left(h_{\mathrm{end,RP}} - 1\right) \exp\left(-\frac{DI}{\tau_{\mathrm{open}}}\right) & \text{if } t^{n+1} \geq T_{\mathrm{act}} + APD + RP \end{cases}$$

$$v_{\mathrm{m}}^{\mathrm{n}+1} = \begin{cases} 1.0 & \text{if } T_{\mathrm{act}} \leq t^{n+1} \leq T_{\mathrm{act}} + APD \\ 0.5 & \text{if } T_{\mathrm{act}} + APD \leq t^{n+1} \leq T_{\mathrm{act}} + APD + RP \\ 0.0 & \text{if } t^{n+1} \geq T_{\mathrm{act}} + APD + RP \end{cases} \tag{14}$$

- If $DI \geq TRR$ the node is marked as re-excitable and is removed from the list of known points (the values $P_{\mathrm{visited}}\left(n_i\right) = \mathrm{false}$), the candidate activation time is set to ∞.

- On points that are marked as excitable, the value of CV is updated

end for on space

Update the activation times between t^n and t^{n+1} following Algorithm 2.

end for on time

Table 1: Tissue properties for the MS model

τ_{in}	τ_{out}	τ_{open}	τ_{close}	v_{gate}
0.3 ms	6 ms	120 ms	150 ms	0.13

5. Numerical Results

In this section, we compare the solutions obtained solving the Eikonal MS model and the monodomain model. We use two different geometries:

- a homogeneous anisotropic tissue slab
- a heart geometry obtained from CT-scan segmentation

The solution of the eikonal model, obtained either with the adaptation of CV to the local electrical state or without adaptation, is compared with the solution obtained from the mono-domain model. For a generic quantity u, the following l_2 relative error norm ($l_{2,\text{r}}$) is defined:

$$l_{2,\text{r}}(u^{\text{eiko}} - u^{\text{mono}}) = \frac{\sqrt{\frac{1}{\text{N}_\text{x}} \sum_{i=1}^{\text{N}_\text{x}} \left(u_i^{\text{eiko}} - u_i^{\text{mono}}\right)^2}}{\sqrt{\frac{1}{\text{N}_\text{x}} \sum_{i=1}^{\text{N}_\text{x}} \left(u_i^{\text{eiko}}\right)^2}}$$

where u_i^{eiko} and u_i^{mono} are the quantities that will be compared, evaluated on the $i-th$ computational node and obtained by solving the monodomain and the eikonal model respectively. On both examples, the monodomain problem is discretized in space with linear finite elements and in time with a first order semi-implicit scheme; the source term characterising the ionic current is treated with an ionic current interpolation, Ethier & Bourgault (2008); Pathmanathan et al. (2012); no mass lumping is applied. On both examples, the ionic parameters characterising the MS ionic model are summarised in Table 1.

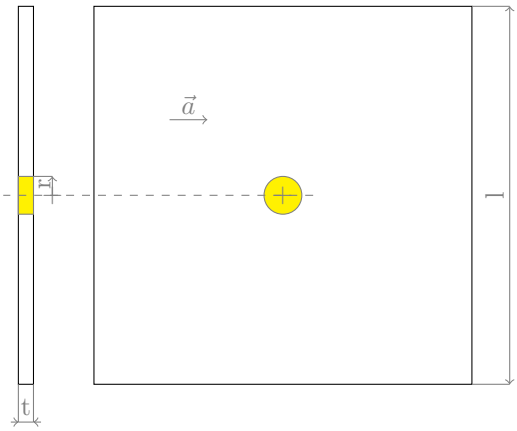

Domain size		
l	r	t
5 cm	0.25 cm	0.1 cm

Figure 1: The $5 \times 5 \times 1\,\mathrm{cm}^3$ tissue slab used in example 1. The yellow region corresponds to the location where the external stimulus is applied. Fibres are oriented along the x direction.

5.1. Tissue slab

The homogeneous tissue slab depicted in Fig. 1 is characterised by a longitudinal conductivity $\sigma_{\mathrm{m}}^{l} = 1.5\,\mathrm{cm}^2/s$ and a transversal conductivity and $\sigma_{\mathrm{m}}^{t} = 0.5\,\mathrm{cm}^2/s$; the fibres $\vec{a}$ are directed along the x direction. The external stimulus is applied on the yellow region in Fig. 1 and with the intensity $I_{\mathrm{app}} = 10\,\mathrm{ms}^{-1}$. The tissue is periodically stimulated by 10 stimuli at a basic cycle length of 400 ms. The monodomain problem is discretized in space with a Delaunay triangulation with a characteristic mesh size h $= 215\,\mu$m, and in time with a time step dt $= 0.01$ ms. The eikonal model is solved on the same mesh and with the same time step, with a value $\delta = 1$, so no graph related correction is introduced to the Dijkstra algorithm.

In Figure 2, two snapshots of the distribution of the transmembrane potential for both monodomain (shadowed) and eikonal model are depicted. The first snapshot is at time 20 ms and the second at time 52 ms. We superimpose both solutions in order to see qualitatively how the wavefronts of both solutions behave. In Figure 3-A we show the time course of the $l_{2,\mathrm{r}}$ error on the transmembrane potential and with respect to the monodomain solution for both the standard eikonal model (red line) and the eikonal model with CV adaptation. When the first stimulus is applied, the tissue is initially at rest, thus $DI \to \infty$,

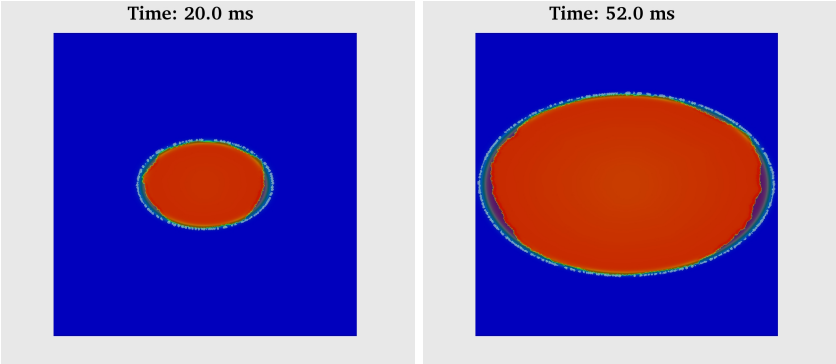

Figure 2: Plot of the eikonal and of the mono-domain (shadowed) solutions for $t = 20$ ms and $t = 52$ ms. The grey contour coincides with the activation front of the monodomain solution. Blue: non activated cells. Red: activated cells.

the value of CV is equal to its maximum and both the models produce the same error. When the subsequent stimuli are applied, h < 1, DI has a finite value and CV adapts according to (5); the eikonal model with the CV adaptation produces a significantly smaller error if compared to the error obtained by solving the standard eikonal model. Moreover, Figure 3-A shows that the $l_{2,\mathrm{r}}$ error decreases during the propagation of the wavefront, reaching its minimum when the slab is fully depolarised. We suppose that the error increasing during the repolarization depends on the absence of the conductivity term since the eikonal model does not play any role after the depolarization; only the ionic model is solved locally at each point of the graph. Whereas, for the monodomain model we still have the influence of the electronic current represented by the diffusion term. The difference between the standard eikonal model and the eikonal model with CV adaptation is much clearer when looking at the error on the activation times. Figure 3-B shows the $l_{2,\mathrm{r}}$ error on the activation times for each of the 10 cycles. Along the 10 cycles, the mean of the $l_{2,\mathrm{r}}$ error on the activation times is 3% when using the eikonal model with CV adaptation, while it is 15.5% when using the standard eikonal model: the velocity the wavefront propagates is indeed much more accurate when using a CV adaptation on the eikonal model.

In Figure 4, the depolarization fronts are plotted for the monodomain model

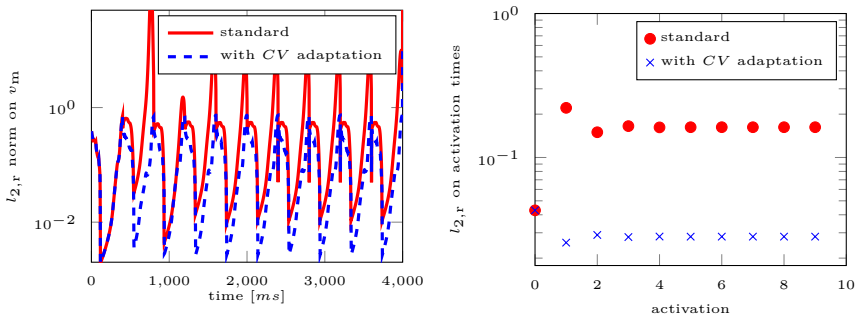

Figure 3: A: Semi-logarithmic plot of the time course of the $l_{2,\mathrm{r}}$ error on the transmembrane potential for the standard eikonal model (red line) and for the eikonal model with CV adaptation (blue line). B: Semi-logarithmic plot of the relative $l_{2,\mathrm{r}}$ error on the activation times at each stimulation for the standard eikonal model (red line) and for the eikonal model with CV adaptation (blue dashed line).

(green dots), the standard eikonal model (red dots) and the eikonal model with CV adaptation (blue dots). The depolarization fronts are plotted at times t=50, 450, 2050 and 3650 ms. At the first cycle (t=50 ms), the depolarization fronts of the eikonal models coincide since the tissue is initially at rest and $DI \to \infty$. From the second applied stimulus (t=450 ms), the depolarization front of the standard eikonal model propagates faster than the monodomain depolarization front; conversely, the depolarization front of the eikonal model with CV adaptation propagates at the same velocity of the monodomain depolarization front. A movie showing the comparison of the depolarization fronts is available in the online supplement.

5.1.1. Oblique fiber direction

In figure 5, we show an example where the fibers are oriented in the diagonal direction of the X-Y plane. The fiber direction in this case is $(\frac{1}{\sqrt{2}}, \frac{1}{\sqrt{2}}, 0)$. We still see that activation time computed with the eikonal model with and without CV adaptation are exactly the same. But from the second heart beat, we see that the speed of the electrical wave in the classical eikonal model is higher than

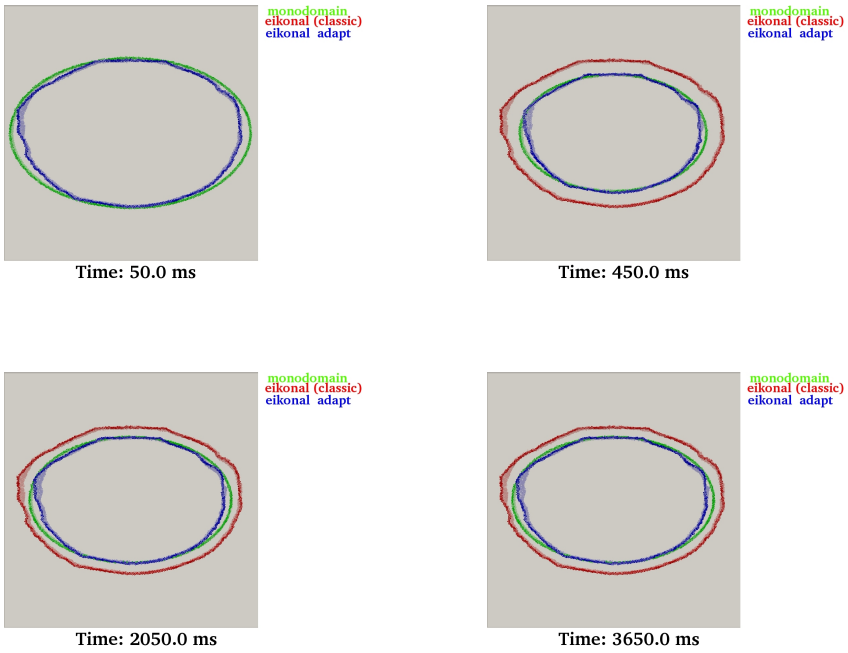

Figure 4: Comparison of wave fronts: Plot of the depolarization front of the monodomain solution (green dots), the standard eikonal solution (red dots) and the eikonal solution with CV adaptation (blue dots). The depolarization fronts are plotted at times t=50, 450, 2050 and 3650 ms.

both CV-adapted and monodomain solution. We also remark that the eikonal solution wave front is less accurate in the regions where the curvature is high. This behavior is also seen in figure 4 where the fiber orientation is given by the X-direction. This is mainly due to the accuracy of the Dijkstra algorithm in the regions where the curvature of the wave front is high and the fact that the Dijkstra solution follows the graph edges.

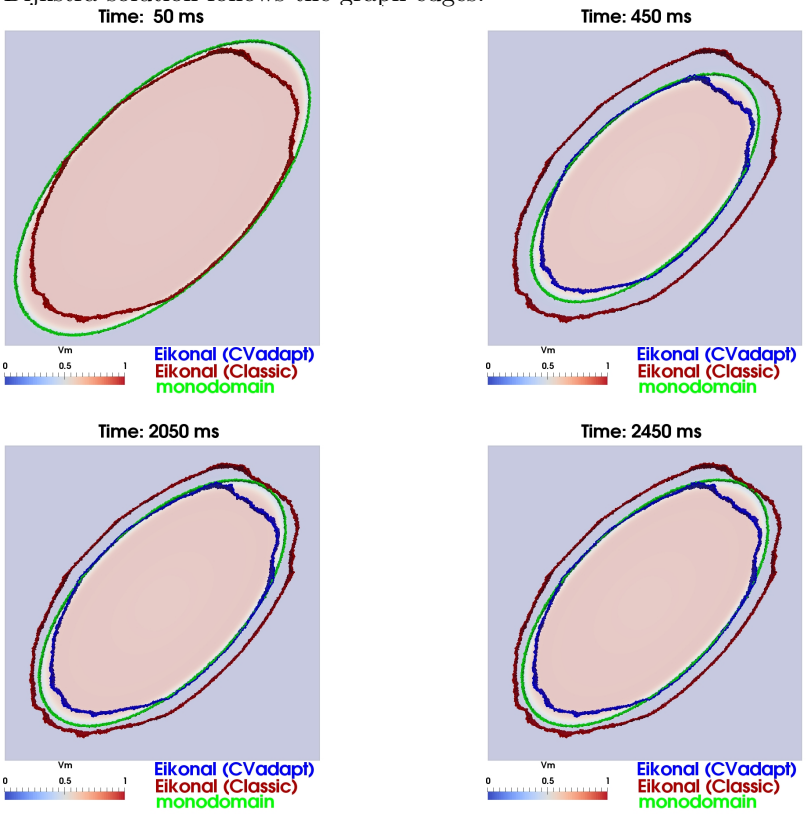

Figure 5: Oblique fiber direction Plot of the depolarization front of the monodomain solution (green dots), the standard eikonal solution (red dots) and the eikonal solution with CV adaptation (blue dots). The depolarization fronts are plotted at times t=50, 450, 2050 and 2450 ms.

5.2. Heart geometry

The geometrical model used in this work was derived from Computerized Tomography (CT) scan data Cardone-Noott et al. (2016) of the human heart. The

initial ventricular mesh, generated with an edge length h $\approx 400\,\mu$m and containing 2.51 million nodes and 14.2 million tetrahedral elements, was re-sampled to $\approx 50,000$ nodes and $\approx 238,000$ tetrahedral elements. The computational mesh is depicted in Figure 6 - A. The fibres and the sheet orientations in the left and

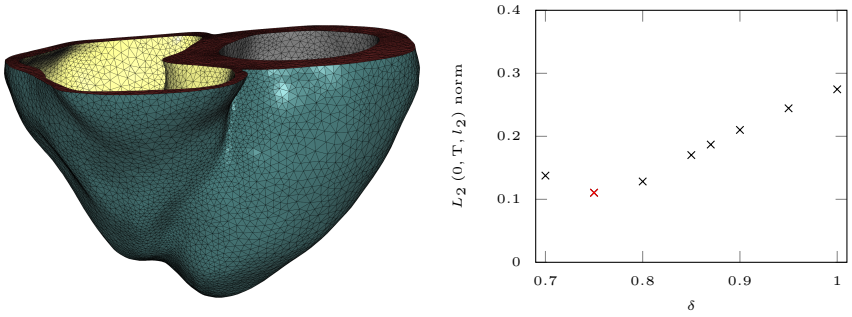

A B

Figure 6: A: Heart geometry discretized using a tetrahedral finite element mesh. B: Plot of the $L_2\,(0,\mathrm{T},l_2)$, $T = 400\,\mathrm{ms}$ norm of the error on the transmembrane potential with respect to the monodomain solution for several values of δ.

right ventricles are depicted in Figure 7 and were generated with the Streeter method Streeter et al. (1979); this method takes into account of the continuous change of the fibre angle across the ventricular wall. The myocardial tissue is characterised by a longitudinal conductivity $\sigma^l_{\mathrm{m}} = 1.5\,\mathrm{cm}^2/s$ and a transversal conductivity $\sigma^t_{\mathrm{m}} = 0.15\,\mathrm{cm}^2/s$.

In this example, an external stimulus is applied at the apex of the left and the right ventricles and with an intensity $I_{\mathrm{app}} = 10\,\mathrm{ms}^{-1}$; the tissue is periodically stimulated by 5 stimuli at a basic cycle length of 400 ms. The problem is discretized in time with a time step dt = 0.01 ms. The eikonal model is solved on the same mesh and with the same time step, and with a corrective coefficient $\delta = 0.75$; this value was determined by first running the eikonal model within the time interval $t = [0, 400]\,\mathrm{ms}$ for several values of δ, then evaluating the $L_2\,(0,\mathrm{T},l_2)$ norm of the absolute error on the transmembrane potential for each value of δ and finally choosing the value yielding the minimum $L_2\,(0,\mathrm{T},l_2)$

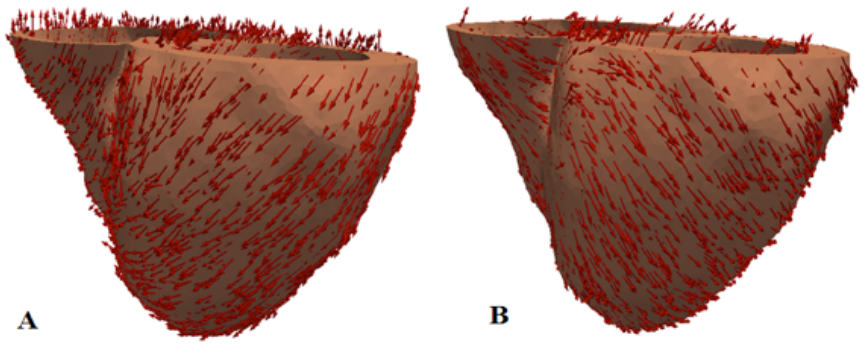

Figure 7: Streeter model generated (A) fibre and (B) sheet direction vectors, mapped on the ventricular geometry.

norm of the error. In Figure 6 - B the $L_2\left(0, \mathrm{T}, l_2\right)$ norm is plotted for several values of δ; on the same figure, the optimal value $\delta = 0.75$ is marked in red. In Figure 8 - A the time course of the $l_{2,\mathrm{r}}$ error on the transmembrane potential is plotted for the standard eikonal model (red line) and the eikonal model with CV adaptation (blue line). When the first stimulus is applied, the tissue is initially at rest, thus $DI \to \infty$, the value of CV is equal to its maximum and both the models produce the same error. When the subsequent stimuli are applied, h < 1, DI has a finite value and CV adapts according to (5); thus, the eikonal model with the CV adaptation produces a significantly smaller error if compared to the error obtained by solving the standard eikonal model. Figure 8 -B shows the $l_{2,\mathrm{r}}$ error on the activation times for each of the 5 cycles. Along the 5 cycles, the mean of the $l_{2,\mathrm{r}}$ error on the activation times is 7% when using the eikonal model with CV adaptation, while it is 18% when using the standard eikonal model. In Figure 9 the depolarization fronts are plotted for the monodomain model (green dots), the standard eikonal model (red dots) and the eikonal model with CV adaptation (blue dots). The depolarization front is tracked by extracting the surfaces where $v_{\mathrm{m}} = v_{\mathrm{gate}}$. The figure highlights the improvements on the accuracy of the eikonal model when CV is adapted to the heart rate. A movie showing the comparison of the depolarization fronts is available in the online

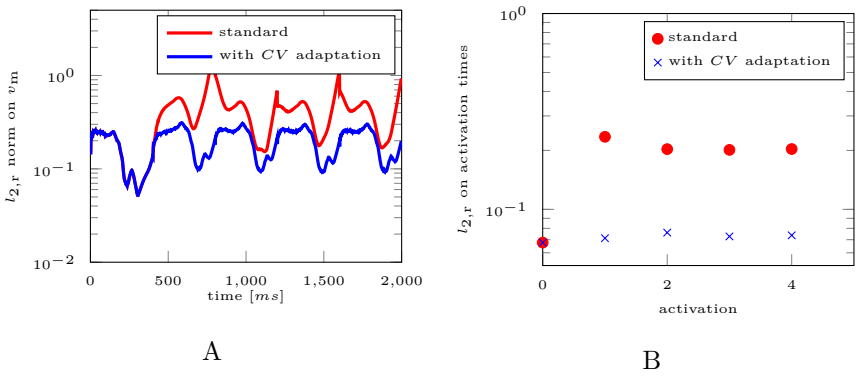

Figure 8: A: Semi-logarithmic plot of the time course of the $l_{2,\mathrm{r}}$ error on the transmembrane potential for the standard eikonal model (red line) and for the eikonal model with CV adaptation (blue line). B: Semi-logarithmic plot of the relative $l_{2,\mathrm{r}}$ error on the activation times at each stimulation for the standard eikonal model (red line) and for the eikonal model with CV adaptation (blue line).

supplement.

6. Discussion

In this paper, we proposed to solve the heart electrophysiology problem by describing the tissue conductivity with an eikonal solver and the ionic activity with an MS ionic model. This proposed approach is suitable for clinical applications where the computational time is the main constraint, particularly if coupled with an efficient algorithm for the local characterization of tissue properties, like the one described in Corrado et al. (2016b). Differently from Pernod et al. (2011); Wallman et al. (2013), in this paper, the eikonal model also takes into account of the local changes in the characteristic propagation velocity and thus is suitable for the simulations of the multi-front propagation and multi-stimuli applications, in particular for the description of the activation pattern characteristic of heart tachyarrhythmias. Despite its simplicity, the chosen ionic model is capable of reproducing the shape of the action potential and the restitution properties of the APD, Mitchell & Schaeffer (2003). For the MS model, it is possible to obtain a leading order approximation of CV and APD restitu-

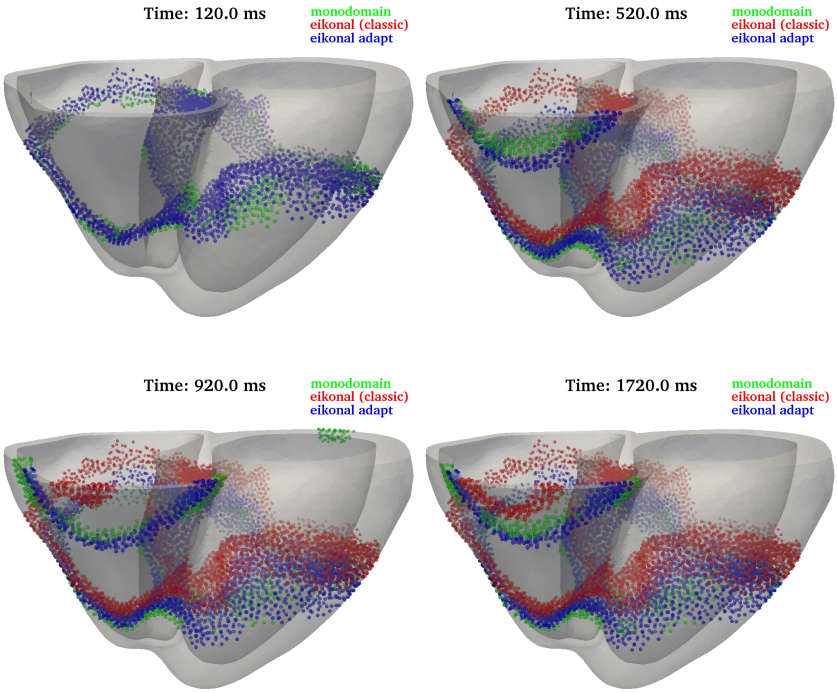

Figure 9: Depolarization fronts at t=120,520,920,1720 ms for the mono-domain model (green dots), the standard eikonal model (red dots) and the eikonal model with CV adaptation (blue dots). The depolarization fronts are tracked as the surfaces where $v_{\mathrm{m}} = v_{\mathrm{gate}}$.

tions, Mitchell & Schaeffer (2003); Cain et al. (2004) as a function of the DI; the approximation on CV was used in this work to adapt the propagation velocity to the underpinning electrical state. However, the approach presented in this work can be used for any characterisation of CV as a function of the history of DI and the action potential duration, or any other quantity related to the computed solution. The current model could be used for the applications presented in Pernod et al. (2011); Wallman et al. (2013), with results that are much closer to the monodomain model. The effects of the CV adaptation become significant when DI decreases; thus, the improved accuracy of the proposed model is significant when high heart rate are considered or regions frequently activated are present.

7. Limitations

The solution of the ionic model is used to determine if a node of the graph is re-excitable and thus allows to reproduce the absolute refractory period (ARP). The solution of the eikonal model furnishes only the time the activation front reaches a node in the graph while its intensity is kept constant and homogeneous within the domain. Since the intensity of the depolarization front affects the propagation of the electrical stimulus during the effective and the relative refractory periods (ERP, RRP), this approximation impacts the ability of the model to capture propagation the failures during refractoriness. A possible solution to overcome this limitation is the matter of a future work. The leading order estimate of the CV restitution, obtained in Cain et al. (2004) and here used to characterise the front propagation velocity, refers to a steady state equilibrium reached when the tissue is stimulated at a constant rate and for a sufficiently long time. Since the MS model does not take into account of any memory effect, the CV adapts instantaneously to the new pacing condition. However, since we lose the diffusion term with the eikonal model with or without CV adaptation, it is more difficult to accurately simulate re-entry waves. The main issue is that the curvature of the wavefront is not well estimated with this model. Hence we don't recommend using this model to study re-entry and in particular spiral waves.

8. Conclusions

We have developed and demonstrated a computational Eikonal Mitchell and Schaeffer model for solving the propagation of the electrical wave in the heart. This model is particularly suitable for applications where the computational time represents the main constraint. This eikonal model adapts the conduction velocity (CV) in the tissue to the activation frequency and thus allows accurately reproducing multi-front activations. Like the monodomain equations, the model here developed allows computing the transmembrane potential and the state variables of the ionic model. The regions of re-excitable tissue are

identified through the computation of the action potential duration and of the diastolic interval (DI). The characteristic propagation speed in the eikonal model is adapted to the electrophysiological state through the analytical CV restitution expression and the computed local DI. Using 3D numerical simulations, we have shown that this model improves the accuracy of tracking the position of the wavefront when compared to the standard eikonal method. This new formulation of the eikonal model is suitable for clinical applications since it is more appealing than the monodomain and bidomain models in terms of computational cost and more accurate than the standard eikonal model.

Aliev, R., & Panfilov, A. (1996). A simple two-variable model of cardiac excitation. *Chaos, Solitons and fractals*, *7*, 293–301.

Cain, J. W., Tolkacheva, E. G., Schaeffer, D. G., & Gauthier, D. J. (2004). Rate-dependent propagation of cardiac action potentials in a one-dimensional fiber. *Physical review E*, *70*, 061906.

Cardone-Noott, L., Bueno-Orovio, A., Mincholé, A., Zemzemi, N., & Rodriguez, B. (2016). Human ventricular activation sequence and the simulation of the electrocardiographic qrs complex and its variability in healthy and intraventricular block conditions. *Europace*, *18*, iv4–iv15.

Clements, J., Nenonen, J., Li, P., & Horacek, B. (2004). Acivation dynamics in anisotropic cardiac tissue via decoupling. *Annals of Biomedical Engineering*, *2*, 984–990.

Corrado, C., Gerbeau, J.-F., & Moireau, P. (2015). Identification of weakly coupled multiphysics problems. application to the inverse problem of electrocardiography. *Journal of Computational Physics*, *283*, 271–298.

Corrado, C., Lassoued, J., Mahjoub, M., & Zemzemi, N. (2016a). Stability analysis of the {POD} reduced order method for solving the bidomain model in cardiac electrophysiology. *Mathematical Biosciences*, *272*, 81 – 91. doi:http://dx.doi.org/10.1016/j.mbs.2015.12.005.

Corrado, C., Whitaker, J., Chubb, H., William, S., Wright, M., Gill, J., O'Neill, M., & Niederer, S. (2016b). Personalized models of human atrial electrophysiology derived from endocardial electrograms. *IEEE Transactions on Biomedical Engineering*, *PP*, 1–1. doi:10.1109/TBME.2016.2574619.

Ethier, M., & Bourgault, Y. (2008). Semi-implicit time-discretization schemes for the bidomain model. *SIAM J. Numer. Anal.*, *46*, 2443–2468.

Kim, J., & Hespanha, J. P. (2003). Discrete approximations to continuous shortest-path: Application to minimum-risk path planning for groups of uavs. In *Decision and Control, 2003. Proceedings. 42nd IEEE Conference on* (pp. 1734–1740). IEEE volume 2.

Luo, C.-h., & Rudy, Y. (1991). A model of the ventricular cardiac action potential. depolarization, repolarization, and their interaction. *Circulation research*, *68*, 1501–1526.

Luo, C.-h., & Rudy, Y. (1994). A dynamic model of the cardiac ventricular action potential. i. simulations of ionic currents and concentration changes. *Circulation research*, *74*, 1071–1096.

Mitchell, C., & Schaeffer, D. (2003). A two-current model for the dynamics of cardiac membrane. *Bulletin Math. Bio.*, *65*, 767–793.

Pathmanathan, P. et al. (2012). Computational modelling of cardiac electrophysiology: explanation of the variability of results from different numerical solvers. *International journal for numerical methods in biomedical engineering*, *28*, 890–903.

Pernod, E., Sermesant, M., Konukoglu, E., Relan, J., Delingette, H., & Ayache, N. (2011). A multi-front eikonal model of cardiac electrophysiology for interactive simulation of radio-frequency ablation. *Computers & Graphics*, *35*, 431–440.

Sermesant, M., Konukoglu, E., Delingette, H., Coudière, Y., Chinchapatnam, P., Rhode, K. S., Razavi, R., & Ayache, N. (2007). An anisotropic multi-front

fast marching method for real-time simulation of cardiac electrophysiology. In F. B. Sachse, & G. Seemann (Eds.), *Functional Imaging and Modeling of the Heart: 4th International Conference, FIHM 2007, Salt Lake City, UT, USA, June 7-9, 2007. Proceedings* (pp. 160–169). Berlin, Heidelberg: Springer Berlin Heidelberg.

Sethian, J. A. (1996). A fast marching level set method for monotonically advancing fronts. *Proceedings of the National Academy of Sciences*, *93*, 1591–1595.

Streeter, D., Berne, R., Sperelakis, N., & Geiger, S. (1979). Gross morphology and fiber geometry of the heart. *Handbook of Physiology, Section 2: The Cardiovascular System*, *1*, 61–112.

Ten Tusscher, K., Noble, D., Noble, P., & Panfilov, A. (2004). A model for human ventricular tissue. *American Journal of Physiology-Heart and Circulatory Physiology*, *286*, H1573–H1589.

Tung, L. (1978). *A bi-domain model for describing ischemic myocardial D–C potentials*. Ph.D. thesis MIT.

Wallman, M., Bueno-Orovio, A., & Rodriguez, B. (2013). Computational probabilistic quantification of pro-arrhythmic risk from scar and left-to-right heterogeneity in the human ventricles. In *Computing in Cardiology Conference (CinC), 2013* (pp. 711–714). IEEE.

Wallman, M., Smith, N. P., & Rodriguez, B. (2012). A comparative study of graph-based, eikonal, and monodomain simulations for the estimation of cardiac activation times. *Biomedical Engineering, IEEE Transactions on*, *59*, 1739–1748.